ChemComm

Accepted Manuscript

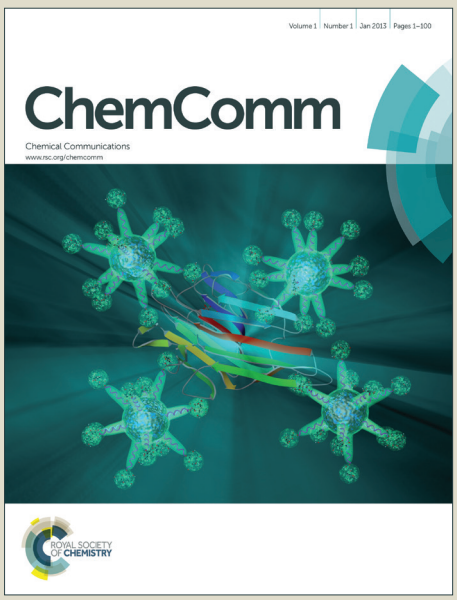

ROYAL SOCIETY OF CHEMISTRY

www.rsc.org/chemcomm

Journal Name

COMMUNICATION

Insight into the formation of magnetite mesocrystals from ferrous precursor in ethylene glycol

Received 00th January 20xx,
Accepted 00th January 20xx

DOI: 10.1039/x0xx00000x

www.rsc.org/

Jiaqi Wan,* Jing Tang, Chongyu Zhang, Ruiting Yuan and Kezheng Chen*

Uniform magnetite mesocrystals were fabricated by solvothermal treatment of ferrous chloride in ethylene glycol in the presence of sodium hydroxide. The formation mechanism of magnetite mesocrystals in ethylene glycol was deduced by a time-dependent experiment.

Mesocrystals, which are defined as an ordered superstructure consisting of crystallographically oriented nanoscale subunits, have received increasing attention in recent years.[1] Mesocrystalline materials offer many potential applications in catalysis,[2] sensing,[3] energy storage and conversion,[4] and life science,[5] owing to their unique characteristics including high crystallinity, high porosity, oriented subunit alignment, and collective properties. In contrast to the classical ion-by-ion addition mechanism of a single-crystal growth, the crystallization pathway of mesocrystals involves mesoscopic transformation of self-assembled, metastable or amorphous precursor particles into highly ordered superstructures.[6] To date, a number of materials with mesocrystalline structures, including metals,[7] metal oxides,[8] organic compounds[9] and biominerals,[10] etc., have been synthesized or discovered in nature. However, it remains a challenging to synthesize mesocrystalline materials with sophisticate architectures, owning to their formation processes are still poorly understood.

Magnetite (Fe_3O_4) nanomaterials have recently been considered an ideal candidate for diverse applications in biomedicine,[11] environmental remediation,[12] and lithium ion batteries[13] etc., owning to their unique properties, low cost, and environmental-friendly nature. After Sugimoto and Matijević reported the preparation of magnetite particles with a narrow size distribution by aging ferrous hydroxide gels in the early 1980s,[14] monodisperse magnetite has been fabricated by various chemistry-based synthetic methods,[15] including coprecipitation, the reverse micelle method, sol-gel techniques, and thermal decomposition. However, most of these approaches focus on magnetite nanoparticles with single-crystalline structure rather than mesocrystalline structure. Recently, Li's group report a general approach for monodisperse ferrite microspheres with obvious mesocrystalline structure by the reaction betw... $FeCl_3 \cdot 6H_2O$ and ethylene glycol under solvothermal conditions, whereas NaAc and polyethylene glycol were simultaneously ad... to assist the transformation of ferric chloride to magnetite an... prevent particle agglomeration.[16] This reaction system has been widely adopted for the fabrication of magnetite superstructures wi... various sizes and morphologies.[17] However, organic additives as well as surfactants make the deduction of mesocrystal formation mechanism complicated.[18] In particular, the change of the valence state and phase transformation of the iron precursor remain open questions.

In this work, we report the reaction of $FeCl_2 \cdot 4H_2O$ in ethylene glycol in the presence of NaOH, which leading to uniform, crystalline, and porous structured Fe_3O_4 mesocrystals. To the best of our knowledge, this is the simplest system for synthetic Fe_3O_4 mesocrystals in ethylene glycol. By employing X-ray diffraction and electron microscopy techniques, we tracked the time-resolved evolution of the iron species and deduced the formation mechanism of magnetite mesocrystals in ethylene glycol.

Fig. 1a presents a typical scanning electron microscopy (SEM) image of the products obtained by solvothermal reaction of $FeCl_2 \cdot 4H_2O$ in ethylene glycol in the presence NaOH at 200 ℃ for 4 hours, which suggests the formation of ~ 300 nm uniform microspheres with rather rough surfaces. The X-ray diffraction (XRD) pattern (Fig. 1b) suggests that the products are pure magnetite (Fe_3O_4) with spinel structure (JCPDS card No. 65-3107). Detailed analysis of the peak broadening of the (311) reflection using the Debye-Scherrer formula indicates an average crystallite grain size of ~23 nm. The difference between the microsphere size and the grain sizes indicates that the magnetite microspheres are composed of smaller building units. Fig. 1c shows a typical TEM image of an individual magnetite microsphere, which confirms that the morphologies of the microspheres are through a dense assembly of the primary particles with recognizable voids or boundaries between the particles. The corresponding selected-area electron diffraction (SAED) of this individual microsphere displays a single-crystalline diffraction pattern with sharp spots along the [114] zone axis of magnetite (inset in Fig. 1c). This ED pattern indicates that the whole microsphere is three-dimensional (3D) assembled by primary particles along the same crystallographic register orientation, w...

College of Materials Science and Engineering, Qingdao University of Science and Technology, Qingdao 266042, China. E-mail: wjiaq@qust.edu.cn, kchen@qust.edu.cn

Electronic Supplementary Information (ESI) available: Experimental details, BET characterization of the magnetite mesocrystals, FT-IR spectra of the iron alkoxide compounds, and TG curves of the precipitates obtained at different reaction time. See DOI: 10.1039/x0xx00000x

is in agreement with the characteristics of mesocrystals. Fig. 1d shows the related high-resolution TEM (HRTEM) image taken from the area marked with a white rectangle in Fig. 1c. The well-resolved lattice fringe of the (311) planes (d=0.256 nm) of magnetite, as highlighted by the Fast Fourier Transforms of the image, further confirms the single-crystalline nature of the whole magnetite superstructure. Moreover, it is clearly seen that the three adjacent primary particles have the same orientation, further confirming that the as-obtained magnetite microspheres are in fact mesocrystals. The porous nature of the as-obtained magnetite mesocrystals is confirmed by nitrogen sorption measurements, which giving rise to a BET surface area of 15 m^2 g^{-1}. (Fig. S1). Thus, uniform magnetite mesocrystals with high-crystallinity and high-porosity were readily fabricated by solvothermal treatment of ferrous chloride and sodium hydroxide in ethylene glycol.

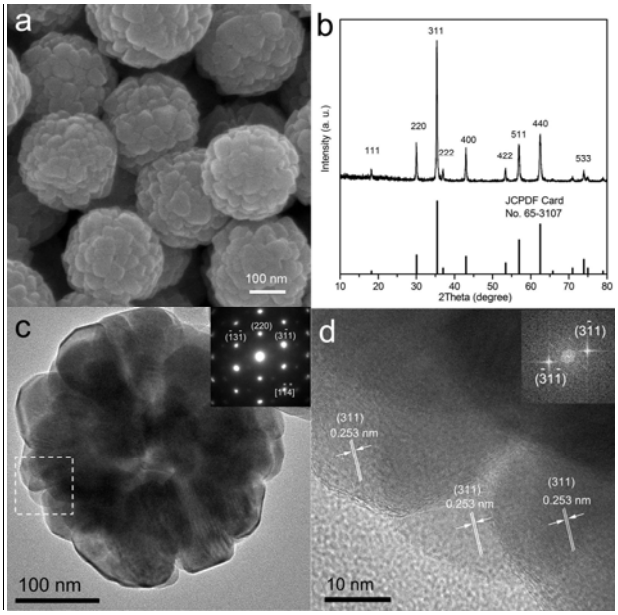

Fig. 1 (a) SEM image and (b) XRD pattern of magnetite mesocrystals. (c) TEM of a single magnetite mesocrystal and its SAED pattern (inset). (d) HRTEM image taken of the area marked with a white rectangle in pane (c) and its FTT pattern.

To obtain a better understanding of the formation mechanism of the magnetite mesocrystals, a time-dependant experiment was carried out. The simplification and moderate crystal growing speed of the reaction system make it possible to spatiotemporally examine the evolution of the involved iron species. Fig. 2 shows the XRD patterns and SEM images of the precipitates obtained at different intervals of the reaction time. As the XRD patterns shown in Fig. 2a, with a shortened reaction of ~10 min, the obtained gray precipitates shows a sharp diffraction peak at 8.442º and broad asymmetric diffraction peaks at 34.5º and 61.6º. The sharp diffraction peak at small Bragg angle is similar to those reported for iron alkoxides with a lamellar structure,[19] whereas the two asymmetric diffraction peaks at high Bragg angles are in agreement with those described for two-line ferrihydrite.[20] The SEM image (Fig. 2b) shows that the products are irregular nanoplatelets with sizes of 100~200 nm, which consist with iron alkoxide compounds with a lamellar structure.[19] Increasing reaction time to 30 min, the metallic Fe phase and Fe_3O_4 phase were simultaneously appeared. From SEM image (Fig. 2c) it can be seen that large amount of Fe_3O_4 microspheres with sizes of 100~200 nm coexist with iron alkoxide compounds. A few ~80 nm nanocubes with sharp facets and edges among the Fe_3O_4 microspheres should be metallic Fe with bcc structure.[21] After reaction for 1 hour, the iron alkoxide and ferrihydrite intermediate phases vanished (Fig. 2a). After 2 hours, metallic Fe phase also vanished and left only pure magnetite phase. Further extending the duration of the reaction, barely increased the crystallinity and grain size, and no new phase appeared. From Fig. 2b-f it can be seen that with the reaction time extending the sizes of the Fe_3O_4 mesocrystals increase gradually. At the same time, the sizes become more uniform and the surfaces are rougher. It is evident that the growth of Fe_3O_4 mesocrystals accomplished by consuming of the sheet-liked iron alkoxide compounds. Therefore, it is believed that the iron alkoxide compounds play a crucial role in the formation of the magnetite mesocrystals.

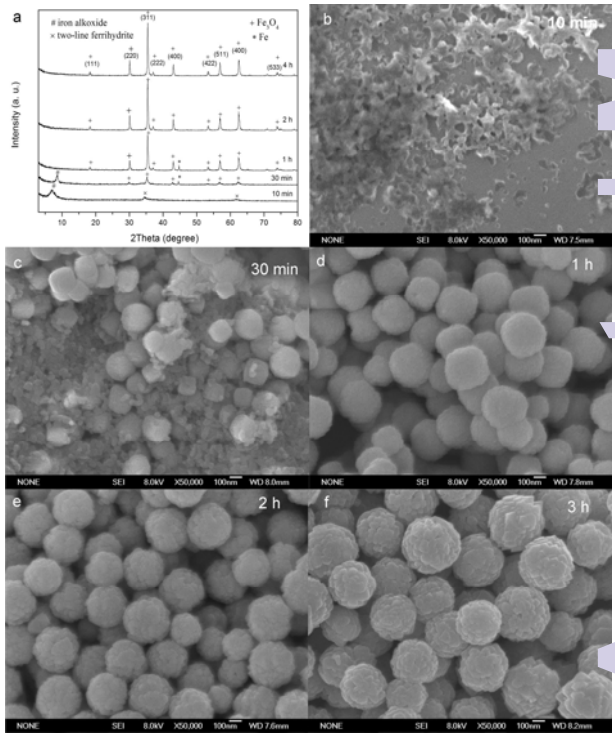

Fig. 2 (a) XRD patterns and (b-f) SEM images of the precipitates obtained at different reaction time from 10 min to 3 h by reaction of $FeCl_2{\cdot}4H_2O$ and NaOH in ethylene glycol at 200 ℃.

The morphology and microstructure of the alkoxide compounds were further examined by TEM and TRTEM. Fig. 3a shows a typical TEM image of the iron alkoxide compounds obtained at 10 minutes. It can be seen that the products are approximately irregular- or hexagonal-shaped thin platelets with sizes of 100~200 nm, which are similar to those previously observed for Co and Ni alkoxide compounds.[22] Fig. 3b shows a HRTEM image of the alkoxide compounds at 10 minutes. Interestingly, it can be found that a host of primer particles with size ~2 nm embodied in the alkoxide matrixes. These primer particles are crystallographic random oriented in the alkoxide platelets, suggesting that the phase transformation occurs at multiple sites within alkoxides in situ. The SAED pattern (Fig. 3b inset) of these primer particles exhibit two apparent diffraction rings at ~0.25 and ~0.15 nm, indicating the sample consists mostly of two-line ferrihydrite.[20] When the reaction

duration was prolonged to 30 minutes, it can be found from the corresponding HRTEM image (Fig. 3c) that the ferrihydrite primer particles embedded in alkoxides were developed denser and the lattice fringes can be observed more clearly. The corresponding SAED pattern (Fig. 3b inset) shows three identifiable diffraction rings at ~0.25, ~0.21 and ~0.15 nm, characteristic of the structures of both ferrihydrite and magnetite. Fig. 3d shows the coexistence of the nascent magnetite mesocrystals and the layered iron alkoxide compounds at the reaction time of 30 min. At this intermediate stage, it can be seen that the nascent magnetite mesocrystals have a relatively rough surface, apparently building from primary particles with the diameter of ~2 nm, similar to those of the ferrihydrite primary particles. Therefore, we hypothesize that the nascent magnetite mesocrystals are constructed and transformed from the ferrihydrite primary particles. This is consistent with the recently observations by Baumgartner et al., which showing that the nucleation and growth of magnetite in alkaline aqueous solution proceed through rapid agglomeration of nanometric ferrihydrite intermediate phase in the presence of ferrous ions.[23] The HRTEM image (Fig. 3d inset) shows that all subunits in this area have the same parallel lattice fringes. The related Fast Fourier Transform (FTT) reflection and SAED patterns (Fig. 3d inset) both exhibit a single-crystal pattern corresponding to magnetite phase, suggesting that the primary particles in the aggregate orient themselves along the same crystallographic orientation. The diffraction spots of the SAED pattern of these nascent mesocrystals are slightly elongated, indicating a small lattice mismatch between the boundaries of the primary particles, typical for mesocrystals.

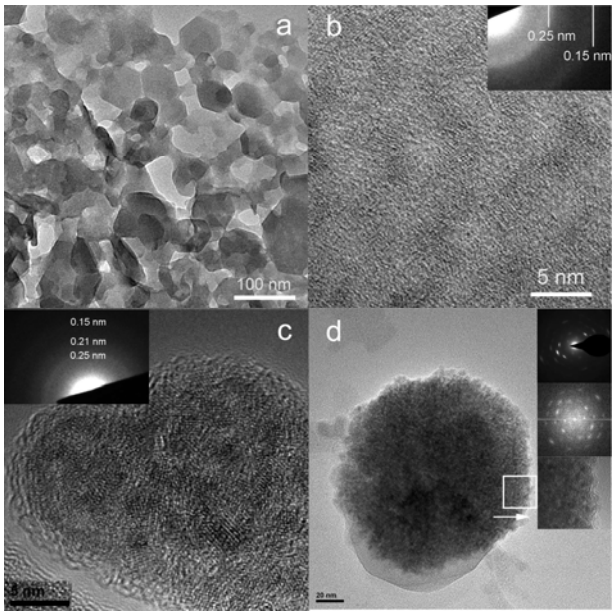

Fig. 3 (a) TEM image of the iron alkoxide compounds obtained at 10 minutes. (b) HRTEM image of a part of the iron alkoxide compounds obtained at 10 minutes. Inset shows the corresponding SAED pattern. (c) HRTEM image of the iron alkoxide compounds obtained at 30 minutes. Inset shows the corresponding SAED pattern. (d) TEM, HRTEM, FTT, and SAED of the nascent magnetite mesocrystals obtained at 30 minutes.

From these observations, we suggest that the formation mechanism of magnetite mesocrystals in the present system may arise as follows. Upon $FeCl_2 \cdot 4H_2O$ and NaOH dissolved in ethylene glycol, Fe^{2+} and OH^- first formed $Fe(OH)_2$ with layered brucite-type structure.[24] The $Fe(OH)_2$ sheets became positively charged wi partial Fe^{2+} ions were isomorphously substituted by Fe^{3+} at elevate temperature, which mainly occurred through oxidation of Fe^{2+} by th residual oxygen. Then the positive charges in the $Fe(OH)_2$ she were balanced by the deprotonated ethylene glycol anio intercalated between the sheets, leading to iron alkoxide compounds with a lamellar turbostratic structure (Fig. 3a).[22, 25] The presence ethylene glycol in alkoxide compounds was evidenced by infrare spectroscopy (Fig. S2) and thermogravimetry (TG) analysis (Fi S3), while the exact crystal structure remains unclear.

The ferrous phases in the alkoxide compounds are sensitive oxidation and can undergo a disproportionation reaction under anaerobic condition, by which the Fe^{2+} phases simultaneously decompose into Fe^0 and Fe^{3+} species.[26] As a result, metallic F phases are observed at the reaction time from 30 minutes to 1 hour (Fig. 2a). Due to the metallic Fe phases can further react with wat by reaction $Fe+2H_2O \rightarrow Fe(OH)_2+H_2$ under anaerobic conditions, they can vanished from the system after 2 hours reaction. Metalli has been observed by Zhang et al. in Li's system[16] at early reaction stage,[18] indicating that the transformation of ferric chloride magnetite in ethylene glycol maybe follow the same reaction pathway.

The ferric ions have a low solubility in alkaline conditio Owning to oxidized by the residual oxygen and disproportionation reaction, more and more ferrous phases converted to ferric phase When the ferric phases became supersaturated with respect to ferrihydrite, most of ~2 nm ferrihydrite nanoparticles formed with the alkoxide matrix in situ through solid-state phase transformatio (Fig. 3a and 3b). It is well-known that the nanometric ferrihydrite have poor structural organization[28] and can quasi-immediately transform into magnetite phase by adsorption of Fe^{2+} ions.[24, 29] In th alkoxide matrix, both ferrihydrite and ferrous phases were temporary stabilized by the ethylene glycol anions, due to their stron coordination ability,[30] which delayed the transformation of ferrihydrite into magnetite phase. As the reaction proceeding, mo NaOH reacted with ethylene glycol giving more water molecules. Upon most ethylene glycol ligands were replaced by wa molecules, both ferrihydrite nanoparticles and ferrous ions becam free to remove. This triggered fast restructuring of nanometric ferrihydrites into ~2 nm magnetite nanoparticles. These magnetite primary particles have a high reactivity due to their large surface fre energy and rich in coordination unsaturated sites. The Brownia motion allows the adjacent primary magnetite particles rotated to find the low-energy configuration by sharing a commo crystallographic orientation.[31] Subsequently, interface eliminatio and reconstruction further reduces overall energy. Finally, temporary equilibrium was established when the tendency toward oriented aggregation, driven by the decrease in surface energy, w counterbalanced by the energy barrier imposed by the electrostatic repulsion.[32] Owing to all the primary particles have the same nature, the resulting superstructures must adopt the same morphology at the equilibrium point. Subsequently, these uniform nascent magnetite mesocrystals underwent a locally dissolution-crystallization proces to further eliminate mismatch defects and interfaces, resulting in high-crystallinity and high-porosity mesocrystalline superstructures.

In conclusion, monodisperse magnetite mesocrystals we synthesized through the reaction of ferrous chloride and sodium hydroxide in ethylene glycol without any other organic additives b one-step solvothermal approach. This reaction offers an excel

model system to understand the mesocrystal formation in ethylene glycol solution owning to its simplification and moderate reaction rate. By conducting a time-resolved experiment, we showed that a lamellar structured iron alkoxide compound first formed, in which positive charged Fe^{3+} isomorphously substituted brucite type $Fe(OH)_2$ is balanced by ethylene glycol anion intercalation. Then a host of ferrihydrite primary particles occurred locally within the alkoxide matrix probably by oxidation and disproportionation reaction. The nanometric ferrihydrites transform into magnetite primary particles by adsorption of ferrous ions. Finally, magnetite mesocrystals formed by oriented aggregation of magnetite primary particles into ordered superstructures and gradual elimination mismatch defects and interfaces. This reaction pathway is similar to that recently found in magnetite crystallization in aqueous solution,[23] and provide a mechanistic insight into mesocrystalline materials formation in non-aqueous solution systems.

This work is supported by the National Natural Science Foundation of China (No. 51472113) and the Natural Science Foundation of Shandong Province (No. ZR2013EMM006).

Notes and references

1 (a) H. Cölfen and M. Antonietti, *Angew. Chem., Int. Ed.*, 2005, **44**, 5576; (b) L. Zhou and P. O'Brien, *J. Phys. Chem. Lett.*, 2012, **3**, 620; (c) M.-G. Ma and H. Cölfen, Current Opinion in Colloid & Interface Science, 2014, **19**, 56; (d) P. Zhang, T. Tachikawa, M. Fujitsuka and T. Majima, *Chem Commun*, 2015, **51**, 7187.

2 Z. Bian, T. Tachikawa, P. Zhang, M. Fujitsuka and T. Majima, *J. Am. Chem. Soc.*, 2013, **136**, 458.

3 (a) X. Hu, J. Gong, L. Zhang and J. C. Yu, *Adv. Mater.*, 2008, **20**, 4845; (b) S. Deng, V. Tjoa, H. M. Fan, H. R. Tan, D. C. Sayle, M. Olivo, S. Mhaisalkar, J. Wei and C. H. Sow, *J. Am. Chem. Soc.*, 2012, **134**, 4905.

4 (a) T. Tachikawa and T. Majima, *NPG Asia Materials*, 2014, **6**, e100; (b) E. Uchaker and G. Cao, *Nano Today*, 2014, **9**, 499.

5 (a) J. Seto, Y. Ma, S. A. Davis, F. Meldrum, A. Gourrier, Y.-Y. Kim, U. Schilde, M. Sztucki, M. Burghammer and S. Maltsev, *Proc. Natl. Acad. Sci. U. S. A.*, 2012, **109**, 3699; (b) L. Bergström, E. V. Sturm, G. Salazar-Alvarez and H. Cölfen, *Acc. Chem. Res.*, 2015, **48**, 1391.

6 (a) R. Q. Song and H. Cölfen, *Adv. Mater.*, 2010, **22**, 1301; (b) M. Niederberger and H. Cölfen, *Physical Chemistry Chemical Physics*, 2006, **8**, 3271; (c) H. Cölfen and S. Mann, *Angew. Chem., Int. Ed.*, 2003, **42**, 2350.

7 J. Fang, B. Ding and H. Gleiter, *Chemical Society Reviews*, 2011, **40**, 5347.

8 (a) Z. Liu, X. Wen, X. Wu, Y. Gao, H. Chen, J. Zhu and P. Chu, *J. Am. Chem. Soc.*, 2009, **131**, 9405; (b) J. Ye, W. Liu, J. Cai, S. Chen, X. Zhao, H. Zhou and L. Qi, *J. Am. Chem. Soc.*, 2010, **133**, 933; (c) X. Duan, L. Mei, J. Ma, Q. Li, T. Wang and W. Zheng, *Chem Commun*, 2012, **48**, 12204

9 Y. Ma, H. Cölfen and M. Antonietti, *J. Phys. Chem. B*, 2006, **110**, 10822.

10 (a) A.-W. Xu, Y. Ma and H. Cölfen, *J Mater Chem*, 2007, **17**, 415; (b) A. W. Xu, M. Antonietti, H. Cölfen and Y. P. Fang, *Adv. Funct. Mater.*, 2006, **16**, 903; (c) A.-W. Xu, M. Antonietti, S.-H. Yu and H. Cölfen, *Adv. Mater.*, 2008, **20**, 1333; (d) S.-S. Wang, A. Picker, H. Cölfen and A.-W. Xu, *Angew. Chem., Int. Ed.*, 2013, **52**, 6317.

11 (a) S. Laurent, D. Forge, M. Port, A. Roch, C. Robic, L. V. Elst and R. N. Muller, *Chem Rev*, 2008, **108**, 2064; (b) D. Ling, N. Lee and T. Hyeon, *Acc. Chem. Res.*, 2015.

12 B. I. Kharisov, H. V. Rasika Dias, O. V. Kharissova, V. Manuel Jimenez-Perez, B. Olvera Perez and B. Munoz Flores, *RSC Advances*, 2012, **2**, 9325.

13 (a) Y. Wang, L. Zhang, X. Gao, L. Mao, Y. Hu and X. W. Lou, *Small*, 2014, **10**, 2815; (b) L. Zhang, H. B. Wu and X. W. Lou, *Advanced Energy Materials*, 2014, **4**, DOI: 10.1002/aenm.201300958.

14 T. Sugimoto and E. Matijević, *J. Colloid Interface Sci.*, 1980, **74**, 227.

15 M. Willard, L. Kurihara, E. Carpenter, S. Calvin and V. Harris, *International Materials Reviews*, 2004, **49**, 125.

16 H. Deng, X. Li, Q. Peng, X. Wang, J. Chen and Y. Li, *Angew. Chem., Int. Ed.*, 2005, **117**, 2782.

17 (a) J. Liu, Z. Sun, Y. Deng, Y. Zou, C. Li, X. Guo, L. Xiong, Y. Ga… F. Li and D. Zhao, *Angewandte Chemie*, 2009, **121**, 5989; (b) … Ge, Y. Hu, M. Biasini, W. P. Beyermann and Y. Yin, *Angew. Chem., Int. Ed.*, 2007, **46**, 4342; (c) P. Hu, L. Yu, A. Zuo, C. Gu… and F. Yuan, *J. Phys. Chem. C*, 2008, **113**, 900; (d) B. Jia and … Gao, *J. Phys. Chem. C*, 2008, **112**, 666; (e) S. Liu, R. Xing, F. L… R. K. Rana and J.-J. Zhu, *J. Phys. Chem. C*, 2009, **113**, 21042.

18 T. Fan, D. Pan and H. Zhang, *Industrial & Engineering Chemistry Research*, 2011, **50**, 9009.

19 (a) L. S. Zhong, J. S. Hu, H. P. Liang, A. M. Cao, W. G. Song … L. J. Wan, *Adv. Mater.*, 2006, **18**, 2426; (b) X. Li, B. Zhang, C. Ju, X. Han, Y. Du and P. Xu, *J. Phys. Chem. C*, 2011, **115**, 12350; (c)B. Wang, H. B. Wu, L. Zhang and X. W. Lou, *Angew. Chem., Int. Ed.*, 2013, **52**, 4165.

20 D. E. Janney, J. M. Cowley and P. R. Buseck, *Clays and Clay Minerals*, 2000, **48**, 111.

21 L.-M. Lacroix, N. Frey Huls, D. Ho, X. Sun, K. Cheng and S. Sun, *Nano Letters*, 2011, **11**, 1641.

22 L. Poul, N. Jouini and F. Fiévet, *Chem. Mater.*, 2000, **12**, 3123…

23 (a) J. Baumgartner, A. Dey, P. H. Bomans, C. Le Coadou, P. Fratzl, N. A. Sommerdijk and D. Faivre, *Nat Mater*, 2013, **12**, 310 (b) J. Baumgartner, G. Morin, N. Menguy, T. P. Gonzalez, M. Widdrat, J. Cosmidis and D. Faivre, *Proc. Natl. Acad. Sci. U. S. A.*, 2013, **110**, 14883.

24 J.-P. Jolivet, C. Chanéac and E. Tronc, *Chem Commun*, 2004, 481.

25 (a) D. Larcher, G. Sudant, R. Patrice and J.-M. Tarascon, *Chem. Mater.*, 2003, **15**, 3543; (b) V. Prevot, C. Forano and J. Besse, *Chem. Mater.*, 2005, **17**, 6695.

26 (a) G. Schrauzer and T. Guth, *J. Am. Chem. Soc.*, 1976, **98**, 3508; (b) F. Shipko and D. L. Douglas, *J. Phys. Chem.*, 1956, **60**, 1519; (c) G. Viau, F. Fievet-Vincent and F. Fievet, *J Mater Chem*, 1996, **6**, 1047.

27 (a) J. Filip, F. E. Karlický, Z. k. Marušák, P. Lazar, M. Cernik, M. Otyepka and R. Zbořil, *J. Phys. Chem. C*, 2014, **118**, 13817; (b) E. J. Reardon, R. Fagan, J. L. Vogan and A. Przepiora, *Environmental science & technology*, 2008, **42**, 2420; (c) E. J. Reardon, *Environmental science & technology*, 2005, **39**, 7311.

28 J. Zhao, F. E. Huggins, Z. Feng and G. P. Huffman, *Clays and Clay Minerals*, 1994, **42**, 737.

29 E. Tronc, P. Belleville, J. P. Jolivet and J. Livage, *Langmuir*, 1992, **8**, 313.

30 X. Jiang, Y. Wang, T. Herricks and Y. Xia, *J Mater Chem*, 200…, **14**, 695.

31 (a) R. L. Penn and J. F. Banfield, *Science*, 1998, **281**, 969; (b) … F. Banfield, S. A. Welch, H. Zhang, T. T. Ebert and R. L. Penn, *Science*, 2000, **289**, 751.
(a) H. Zhang, J. J. De Yoreo and J. F. Banfield, *ACS Nano*, 201…, **8**, 6526; (b) A. Bakandritsos, G. C. Psarras and N. Boukos, *Langmuir*, 2008, **24**, 11489; (c) Y. Xia, T. D. Nguyen, M. Yang, B. Lee, A. Santos, P. Podsiadlo, Z. Tang, S. C. Glotzer and N. … Kotov, *Nat. Nanotechnol.*, 2011, **6**, 580.